

Supplemental Information: A multiscale approach to uncover the self-assembly of ligand-covered palladium nanocubes

Xiangyu Chen¹, Thi Vo¹, Paulette Clancy^{1*}

¹Department of Chemical and Biomolecular Engineering, Johns Hopkins
University, Baltimore, MD, 21218, USA

*Corresponding author, email: pclancy3@jhu.edu

We chose the Paul force field over commonly used OPLS force field because OPLS tends to model the alkane ligand as “brush-like” rods instead of interdigitating woven[1, 2]. We tested both Paul and OPLS force field in vacuum and visualized their difference in ligand modeling in Figure 1. It is clear that OPLS force field modeled dodecanethiol as “stiff” molecules standing up straight and Paul force field model them as interlacing molecules. We ran the comparison at 298, 325, 373 K and the difference persisted.

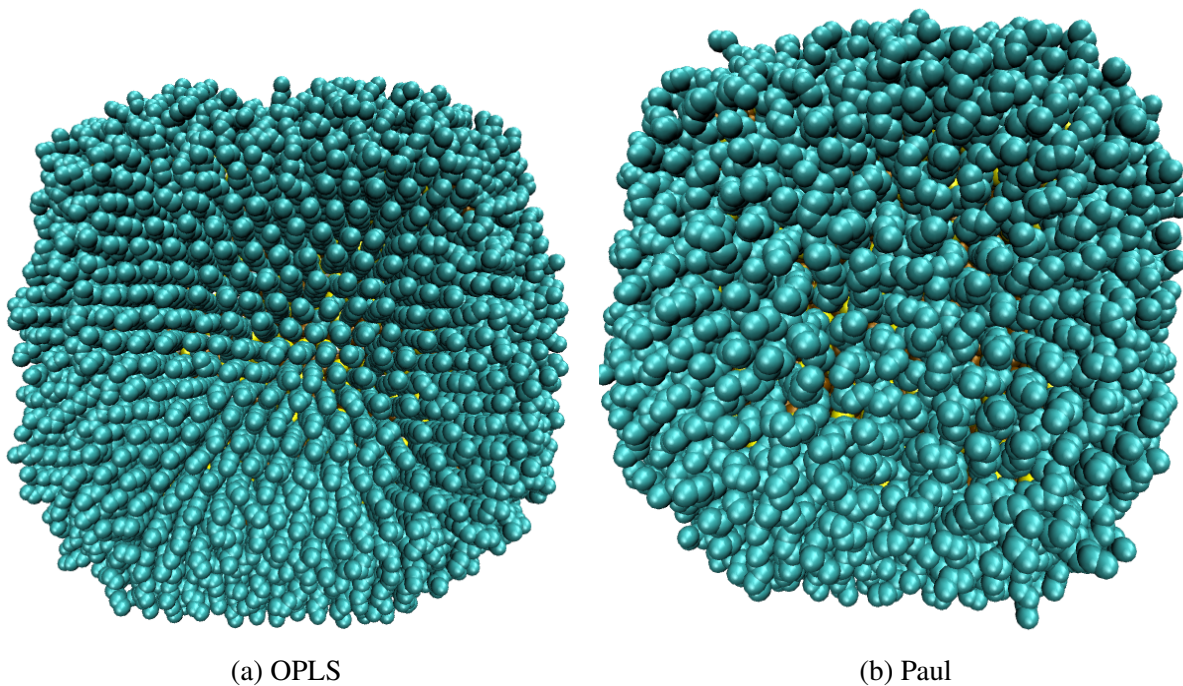


Figure S1: Visualization of dodecanethiol covered palladium nanoparticle using OPLS force field (a) and Paul force field (b) at room temperature.

Table S1: Harmonic bond parameter for palladium - sulfur[1]

	k (kcal/mol/Å ²)	r_0 (Å)
Pd-S	265	2.4

Table S2: 12-6 Lennard-Jones parameters for Palladium atoms in a face-centered particle[3]

	ϵ (kcal/mol)	σ (Å)
Pd	6.15	2.512

Table S3: 12-6 Lennard-Jones parameters of ligand molecule in opti-mized united-atom model for simulations of polymethylene melts

	ϵ (kcal/mol)	σ (Å)
CH ₃	0.22644	4.009
CH ₂	0.09344	4.009
SH	0.3	4.25

Table S4: Bond parameters of ligand molecule in optimized united-atom model for simulations of polymethylene melts

Harmonic bond interaction	k (kcal/mol)	r_0 (Å)
C-C bond	444	1.81
S-C bond	643	1.53

Table S5: Angle and dihedral parameters of ligand molecule in optimized united-atom model for simulations of polymethylene melts (k_i is in kcal/mol)[2]

Angle and dihedral interaction	θ_0 (degree)	k_1	k_2	k_3
C-C-C angle	110.01	120	N/A	N/A
S-C-C angle	113.4	125	N/A	N/A
C-C-C-C dihedral	N/A	1.6	-0.867	3.24
S-C-C-C dihedral	N/A	1.6	-0.867	3.24

Table S6: 12-6 Lennard-Jones parameters of toluene seven point united-atom model of TraPPE-UA force field[4]

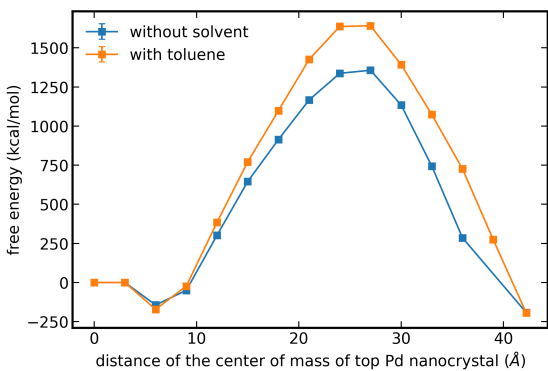
	ϵ (kcal/mol)	σ (Å)
CH (aromatic carbon)	0.1003	3.695
CH-[C]-CH ₃	0.04173	3.88
CH ₃	0.1947	3.75

Table S7: Bond and angle parameters of toluene in united-atom model of TraPPE-UA force field[4]

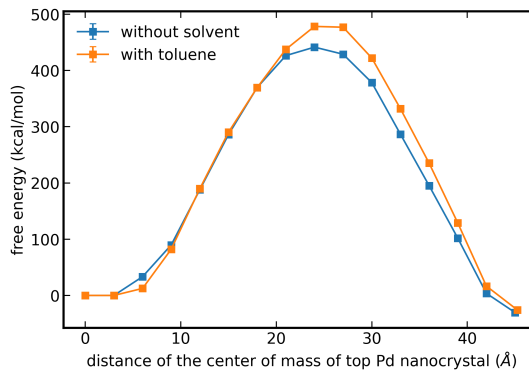
Angle and dihedral interaction	r_0 (Å)	θ_0 (degree)	k (kcal/mol)
CH-CH bond	1.54	N/A	rigid
CH-CH ₃ bond	1.40	N/A	rigid
CH-CH-CH angle	N/A	120	rigid
CH-CH-CH ₃ angle	N/A	120	rigid

Table S8: Free energy barrier of transition from face-to-face to brick-wall configuration in vacuum and toluene. All units are in kcal/mol.

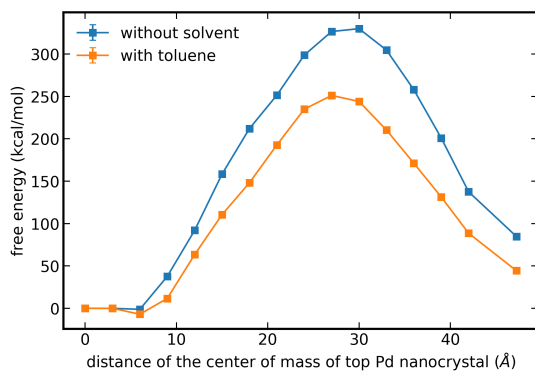
	C-6	C-9	C-12	C-15
Vacuum	1356	441	329	204
Toluene	1641	478	251	N/A



(a) C-6

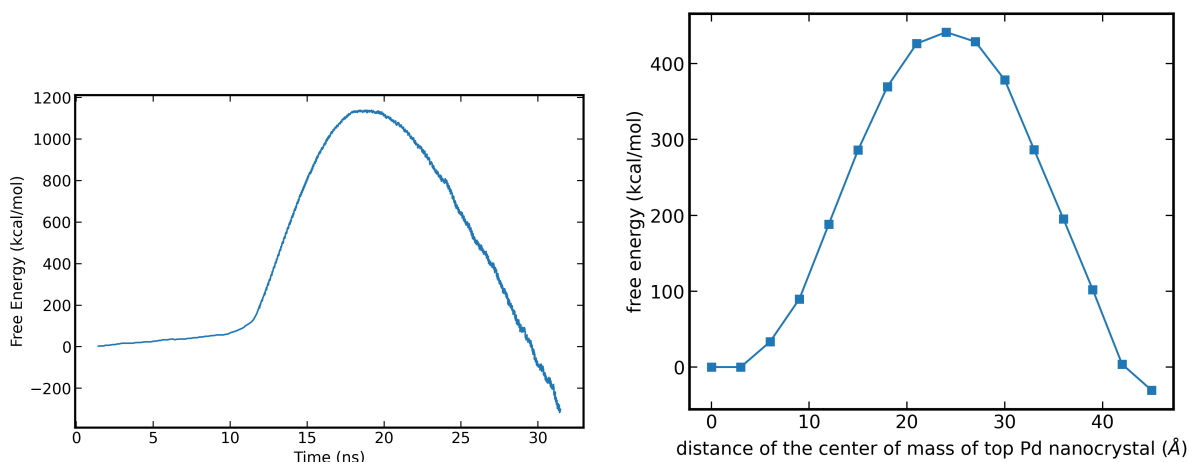


(b) C-9

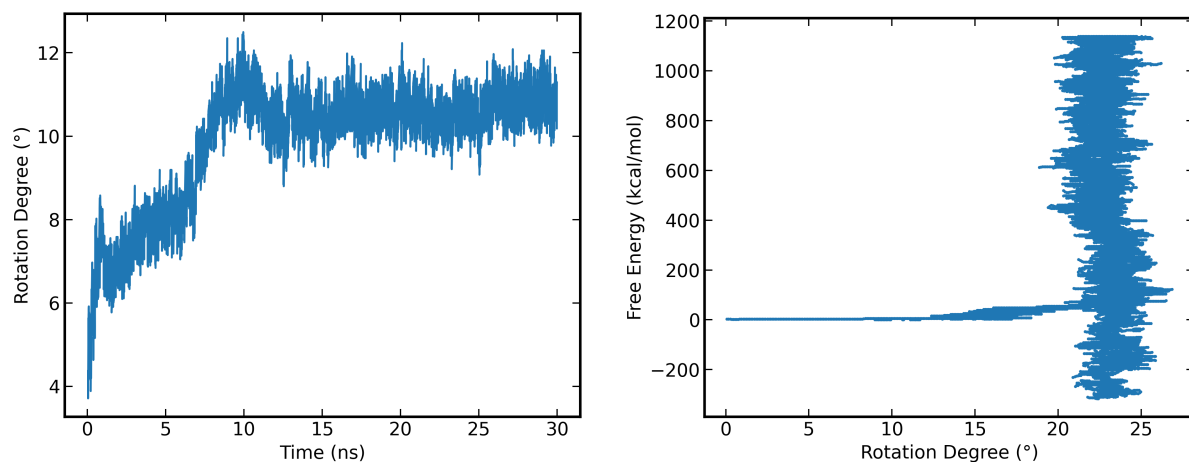


(c) C-12

Figure S2: Comparison of free energy landscapes provided by TI in vacuum (blue) and in a coarse-grained toluene solvent (orange). (a)-(c) show results for C-6, C-9 and C-12 ligands, respectively.



(a) [Left] Steered Molecular Dynamics (SMD) values for the free energy landscape as a function of time. [Right] Corresponding Thermodynamic Integration results for the same process as a function of distance, which are linearly related. The SMD-derived peak at about 20 ns occurs when the system adopts a brick-wall configuration. Note that it is typical for the energy values to differ significantly between SMD and TI, with the latter typically assumed to be more accurate.



(b) [Left] Degree of rotation of the top particle relative to the bottom layer of the Pd particles during SMD simulations for the results shown in Figure 3(a). The particle rotates by $\sim 11^\circ$ at about 10 ns and maintains that tilt throughout the rest of the transition. [Right] Lack of correlation between the degree of rotation of the top particle (shown on the left) and the free energy of the system.

Figure S3: Thermodynamic profiles of the Steered Molecular Dynamic simulation of the configurational change in a 3-nanoparticle system.

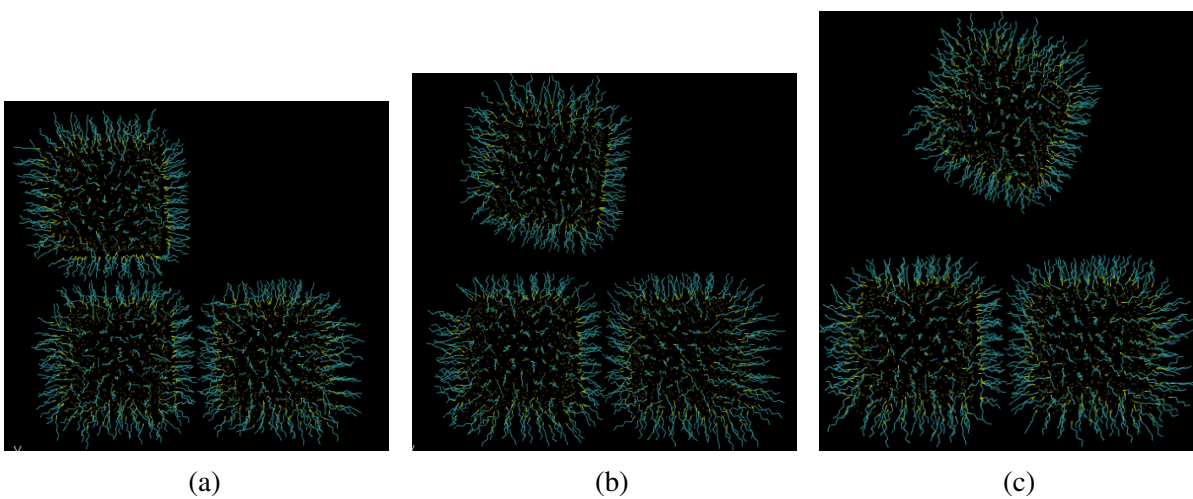


Figure S4: Visualization of the steered Molecular Dynamics simulation trajectory of 3-nanoparticle system undergoes face-to-face to brick-wall configuration change. Palladium atoms are displayed as dots and ligand molecules are displayed as lines.

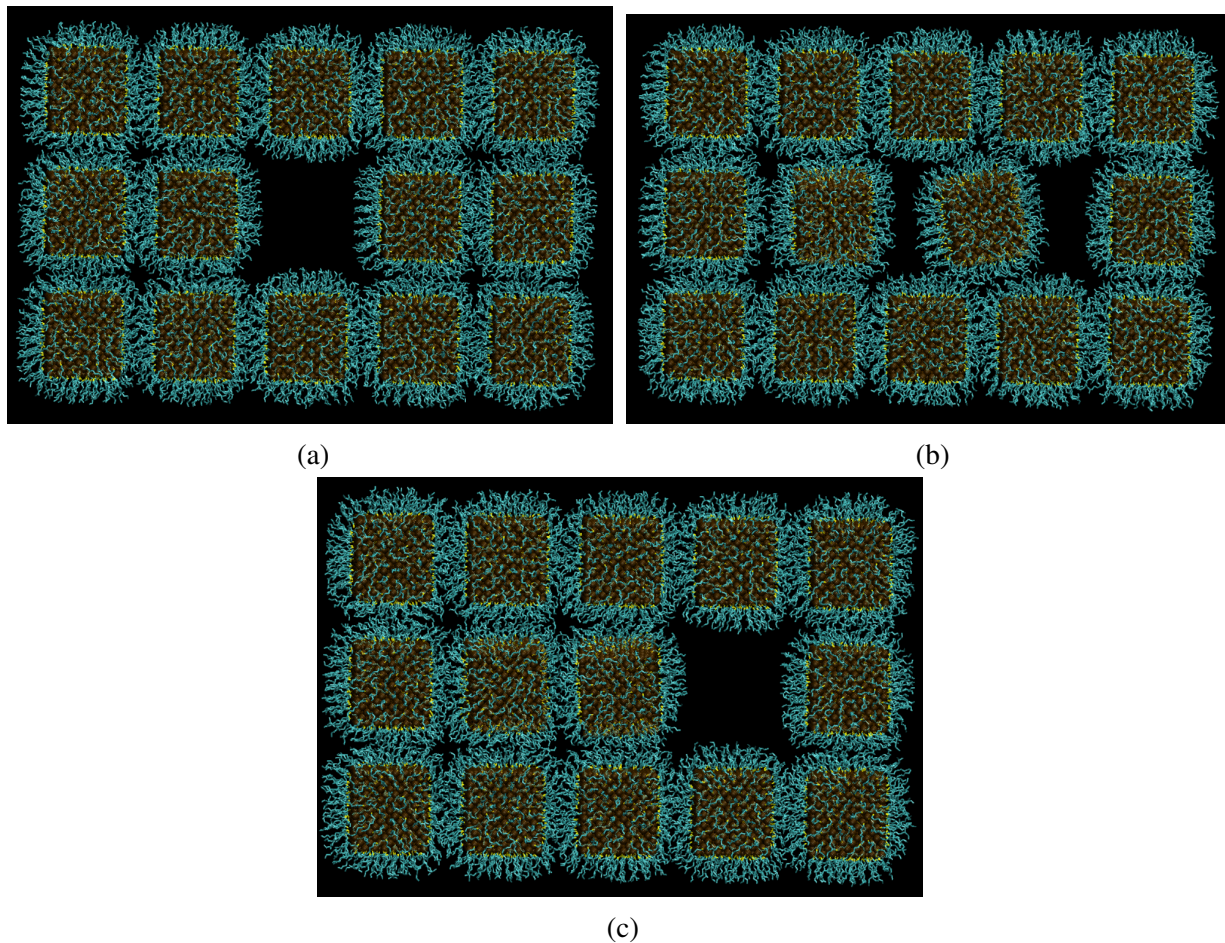
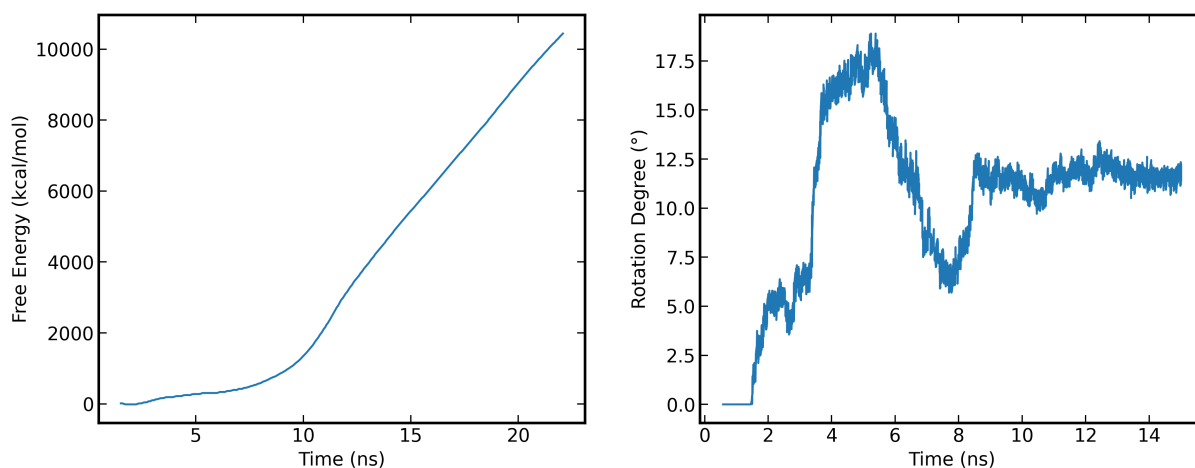
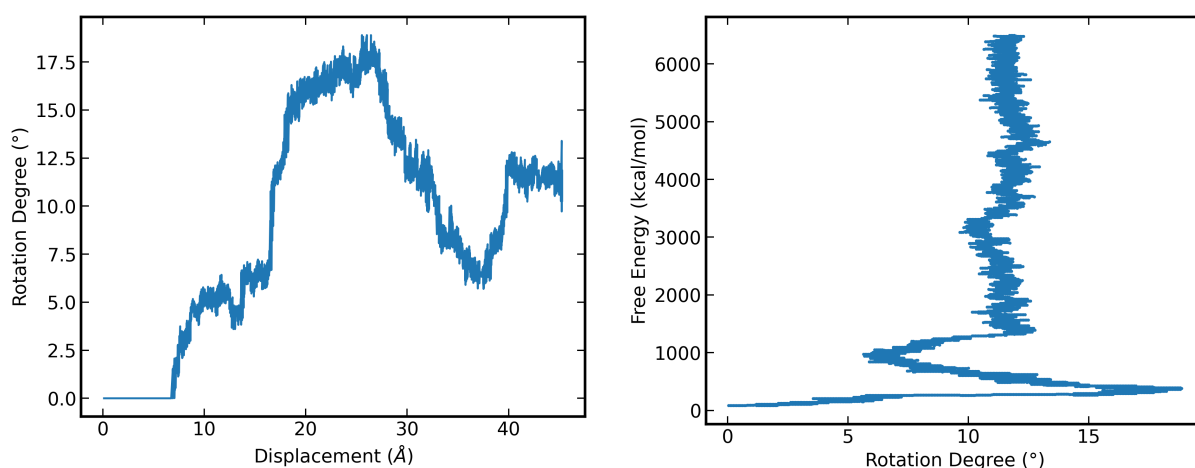


Figure S5: Snapshot of an starting (a), intermediate (b) and the final (c) frame of the simulation of described in Figure 2 in the method section. In (a), the pulled nanoparticle is at the initial face-to-face configuration. In (b), it has arrived at the brick-wall configuration in its local lattice site, exhibiting a $15\text{-}18^\circ$ rotation with respect to the bottom layer of Pd nanoparticles. Note, the movement of the nanoparticle nearest to the moving particle towards the moving nanoparticle. In (c), the pulled nanoparticle has reached its destination but maintained $\sim 11^\circ$ of rotation in spite of the spring force continuing to exist. All solvent molecules are hidden for clarity.



(a) Free energy landscape of the SMD simulation illustrated in Figure 5. The significant increase in free energy reflects the difficulty of overcoming the intermolecular forces needed to continuously pull B towards A.

(b) Rotation of nanoparticle B with respect to the bottom layer of the superlattice as a function of time during the simulation, showing a maximum rotation of 15-18° after 4-6 ns, a time corresponding to the brick wall position. It then returns to a tilt of about 11° as B moves into its final F2F configuration adjacent to A.



(c) Relationship between the degree of rotation and the displacement of nanoparticle B. It shows that the free energy change during the pulling B to the nanoparticle reached a maximum rotation of 15-18° around 20 to 28 Å corresponding to the brick wall configuration. It then returns to a tilt of about 11° as B moves into its final F2F configuration adjacent to A.

(d) Relationship between the degree of rotation and the free energy change during the pulling B to the nanoparticle. It shows that the maximum rotation (~18°) corresponds to the lowest free energy and that the particle remains tilted by about 11° as it returns to the F2F position.

Figure S6: Thermodynamic profiles of the Steered Molecular Dynamic simulation illustrated in Figure 5. Parts (a)-(d) described above.

References

- (1) Kaushik, A. P.; Clancy, P. Solvent-driven symmetry of self-assembled nanocrystal superlattices—A computational study. *Journal of computational chemistry* **2013**, *34*, 523–532.
- (2) Paul, W.; Yoon, D. Y.; Smith, G. D. An optimized united atom model for simulations of polymethylene melts. *The Journal of chemical physics* **1995**, *103*, 1702–1709.
- (3) Heinz, H.; Vaia, R.; Farmer, B.; Naik, R. Accurate simulation of surfaces and interfaces of face-centered cubic metals using 12-6 and 9-6 Lennard-Jones potentials. *The Journal of Physical Chemistry C* **2008**, *112*, 17281–17290.
- (4) Liu, X.; Ni, Y.; He, L. Molecular dynamics simulation of interparticle spacing and many-body effect in gold supracrystals. *Nanotechnology* **2016**, *27*, 135707.